Front. Earth Sci. 2023, 17(3): 867–883
https://doi.org/10.1007/s11707-022-1078-y

RESEARCH ARTICLE

Research on the pressure variation law and enhancing CBM extraction application effect of CO_2 phase transition jet coal seam fracturing technology

Xin BAI (✉)[1,2,3], Zhuoli ZHOU[1], Guicheng HE (✉)[1], Dongming ZHANG[4], Han YANG[4], Zenrui FAN[5], Dengke WANG[2]

1 School of Resources Environment and Safety Engineering, University of South China, Hengyang 421001, China
2 State Key Laboratory Cultivation Base for Gas Geology and Gas Control, Henan Polytechnic University, Jiaozuo 454000, China
3 Key Laboratory of Safety and High-efficiency Coal Mining (Ministry of Education), Anhui University of Science and Technology, Huainan 232001, China
4 School of Resources and Safety Engineering, Chongqing University, Chongqing 400044, China
5 China Coal Technology Engineering Group Chongqing Research Institute, Chongqing 400037, China

Abstract Due to the limited permeability and high methane content of the majority of China's coal seams, significant coal mining gas disasters frequently occur. There is an urgent need to artificially improve the permeability of coalbed methane (CBM) reservoirs, enhance the recovery efficiency of CBM and prevent mine gas accidents. As a novel coal rock fracture technology, the CO_2 phase transition jet (CPTJ) has been widely used due to its advantages of safety and high fragmentation efficiency. In this study, to ascertain the effects of the pressure of CPTJ fracturing, the influence of its jet pressure on cracked coal rock was revealed, and its effect on CBM extraction was clarified. In this research, the law of CPTJ pressure decay with time was investigated using experimental and theoretical methods. Based on the results, the displacement and discrete fracture network law of CPTJ fracturing coal rock under different jet pressure conditions were studied using particle flow code numerical simulation. Finally, field experiments were conducted at the Shamushu coal mine to assess the efficiency of CPTJ in enhancing CBM drainage. The results showed that the pressure of the CPTJ decreased exponentially with time and significantly influenced the number and expansion size of cracks that broke coal rock but not their direction of development. CPTJ technology can effectively increase the number of connected microscopic pores and fractures in CBM reservoirs, strongly increase the CBM drainage flow rate by between 5.2 and 9.8 times, and significantly reduce the CBM drainage decay coefficient by between 73.58% and 88.24%.

Keywords coalbed methane (CBM), CO_2 phase transition jet, pressure evolution, damage of coal, CBM drainage

Received September 3, 2022; accepted February 26, 2023

E-mail: Baixin112@126.com (Xin Bai)
hegc9210@163.com (Guicheng He)

1 Introduction

CBM is a toxic and harmful product in coal mines and is known as the "curse" of coal miners (Byrer et al., 2014). The calorific value of CBM is 34–38 MJ/m^3, which is comparable to the combustion calorific value of natural gas (Flores, 2013; Zhang et al., 2017). Over the past 20 years, CBM has developed into an indispensable energy source in the USA, Russia and Australia (Barnhart et al., 2016). In China, the reserves of CBM resources within 2000 m have been surveyed and proven to be 36.81 trillion m^3 (Qin et al., 2018). However, the permeability of most CBM reservoirs in China is relatively low, which makes CBM extraction difficult and causes frequent mine gas accidents (Zhao et al., 1995; Zhou et al., 2020a, 2021). Therefore, it is urgent to take certain technical measures to improve the permeability of CBM reservoirs (Wang et al., 2012; Wang et al., 2017). Due to the advantage of high efficiency, blast fracturing has been widely applied to CBM reservoir fracturing for a period of time (Yang et al., 2019). Nevertheless, strong energy and shock waves released during the explosive process disturb and damage the buried environment of CBM reservoirs, which affects the stability of the rock mass in the mining operation area to a certain extent

(Dowding et al., 2016; Ainalis et al., 2017). To ensure the security of mine workers, the release of blasting energy should be reduced while achieving the ideal fracturing effect of CBM reservoirs (Jaimes et al., 2012). Under these circumstances, a novel CO_2 phase change jet (CPTJ) fracturing technology for CBM reservoirs may be an alternative method.

Recently, a novel technique has been proposed that involves the use of CPTJ to crack CBM reservoirs. CPTJ technology uses high-pressure gas jets and shock stress wave formed by the phase change of heated liquid CO_2 to act on coal seams and promote an increase in coal fractures (Bai et al., 2020). In earlier studies, a many scholars found that the rock breaking efficiency of CO_2 jets was better than that of water jets (Vishal et al., 2015; Deng et al., 2018; Lu et al., 2022). Furthermore, previous studies clearly showed that coal seams have a stronger adsorption capacity for CO_2 than for methane (Liu et al., 2017; Qin et al., 2021). After CO_2 is injected into a coal seam, under the effect of competitive adsorption, the free gas content in the fractured coal can be increased, thus increasing the flow rate and concentration of coalbed methane drainage (Liu et al., 2019; Cheng et al., 2021a). In particular, as a relatively safe and efficient fracturing technology, CPTJ fracturing technology has generated extensive interest in the field of CBM drainage (Li et al., 2018). Lu et al. (2015) improved the traditional CARDOX system to make it useable for coal seam fracturing and field tested the effect of the application of the improved high-energy CPTJ system. After that, Chen et al. (2017) studied the influence scope of CPTJ coal seam fracturing technology by a numerical research method. Cao et al. (2017) conducted a field test to study the effect of CPTJ coal seam fracturing technology on improving coalbed methane extraction efficiency. Zhang et al. (2018) revealed the expansion mechanism of CPTJ coal seam fractures by theoretical research. Gao et al. (2018) used CO_2 phase transition technology to conduct rock fracture experiments without an initial stress field and obtained a calculation formula for the crack propagation radius under stress waves. Hu et al. (2019) experiments showed that multiple crossed cracks formed in cylindrical concrete specimens under the action of CO_2 caused by instantaneous changes in phase and pressure. After rapid development in recent years, the CPTJ technique was developed into a relatively safe and efficient technology. It is widely used for coal seam permeability enhancement and rock fragmentation.

According to an analysis, most studies have focused on the effect of using CPTJ technology on ECBM, with many reporting favorable results (Hu et al., 2018; Zhou et al., 2020b; Zheng et al., 2022). It was concluded that there are few reports on the decay law of CO_2 jet pressure in the existing CPTJ technology research, especially studies on the theoretical equation of jet pressure change with time under different initial pressures. However, these laws are very important for basic theoretical research and field technology optimization of CPTJ technology. Therefore, it is necessary to study the evolution law of jet pressure under different initial pressure conditions of CPTJ technology and carry out numerical simulations of CPTJ technology coal breaking. In this paper, first, the developed CPTJ coal-rock fracturing experimental system was used to study and clarify the pressure decay law with time under different initial pressure conditions during CPTJ. Then, using fluid mechanics theory and the energy balance law, a theoretical model of CPTJ pressure change with time was established. After that, the particle flow code (PFC) numerical simulation method was used to research the influences of the initial pressure on the distribution characteristics of coal fractures destroyed by CPTJ. Finally, a field experiment was conducted in the Sha Mushu mining area to evaluate the efficiency of CPTJ technology in improving CBM recovery.

2 Experimental equipment and research procedure

2.1 Experimental equipment

2.1.1 CPTJ coal fracturing experimental system

Figure 1 shows a simplified diagram of the CPTJ coal fracturing experimental system (Bai et al., 2020). This apparatus was designed to study the decay law of CPTJ pressure with time and to clarify the effect of CPTJ fracturing in coal rock masses. The principle of this experimental apparatus was to pressurize, liquefy and store gaseous CO_2 by driving a booster pump with high-pressure air until it reaches the set pressure value. Then, the solenoid valve was opened, which caused the pressure of the L-CO_2 in the storage tank to drop sharply, the phase transition occurred instantaneously, the volume expanded by 260 times, forming a high-pressure CO_2 gas jet, and the generated impact stress instantly acted on the coal rock mass sample. In this experimental apparatus, the output pressure of the air compressor was 0.8 MPa; the boosting ratio of the booster pump was 1:100; the volume of the storage tank was 5 L; the maximum pressure that could withstand was 80 MPa; and the diameter of the nozzle was 2.5 mm. At the same time, the gas pressure sensor could be used to measure the gas pressure of the nozzle during CPTJ.

2.1.2 CPTJ coal fracturing ECBM technology equipment

The CPTJ coal fracturing ECBM technology equipment contained a CPTJ coal seam fracturing device, a CO_2 pressurized filling system, and a hydraulic drilling rig, as shown in Fig. 2. This equipment was developed for field testing of CPTJ coal fracturing technology.

During the field application, CO_2 was poured into the high-pressure storage tube using the pressurized filling system described above. Then, the CO_2 storage tube was installed into the drilled hole by a hydraulic drill rig. The

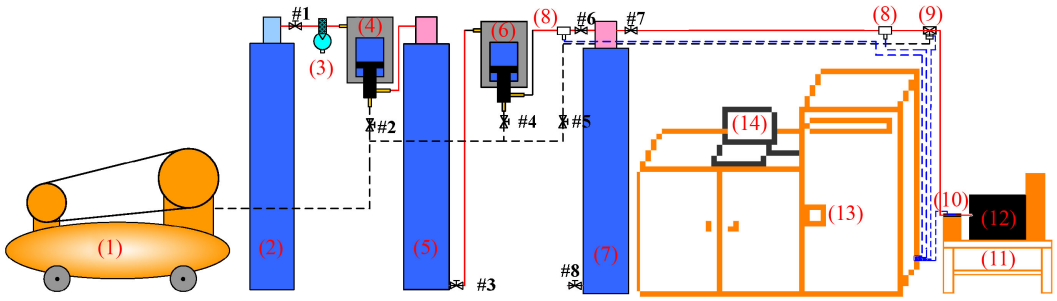

(1) Air compressor (2) CO_2 cylinder (3) Gas-water separator (4) CO_2 gas booster pump (5) L-CO_2 storage tank

(6) L-CO_2 booster pump (7) High pressure L-CO_2 storage tank (8) Pressure sensor (9) CNC pneumatic valve

(10) Jet nozzle (11) Specimen loading device (12) Coal specimen (13) Data collection system (14) Computer

Manual valve CO_2 pipeline High-pressure gas pipeline Data collection line

(a) Schematic diagram of experimental system

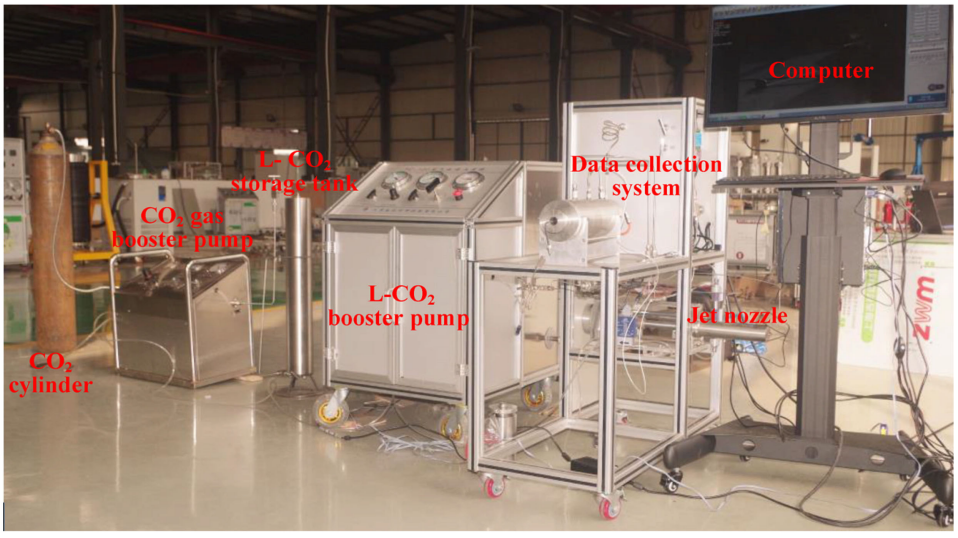

(b) Actual photographic of experimental system

Fig. 1 CPTJ coal fracturing experimental system.

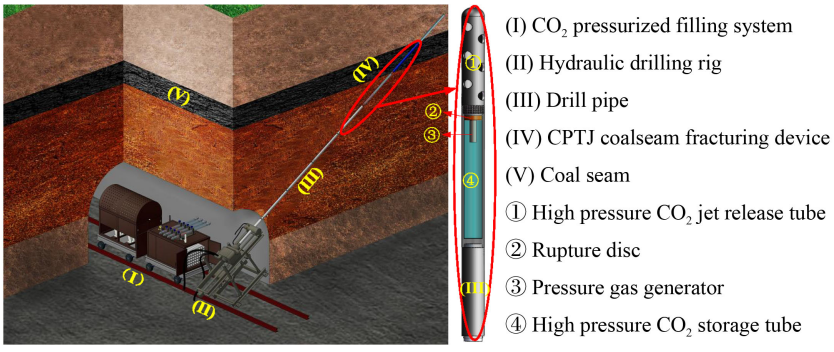

Fig. 2 Schematic diagram of CPTJ coal fracturing ECBM technology equipment.

pressure gas generator in the CO_2 storage tube was activated remotely, causing the thermal expansion of the L-CO_2 in the storage tube to reach the threshold for the rupture disk. The volume-expanded CO_2 gas instantly formed a high-pressure jet from the release tube, which impinged on the coal of the borehole wall to generate cracks.

2.2 Research procedure

The purpose of this research is to obtain the pressure variation law of CPTJ coal seam fracturing technology, reveal the influence of its jet pressure on cracked coal rock, and clarify its enhanced CBM extraction effect. The research scheme of this study is shown in Fig. 3.

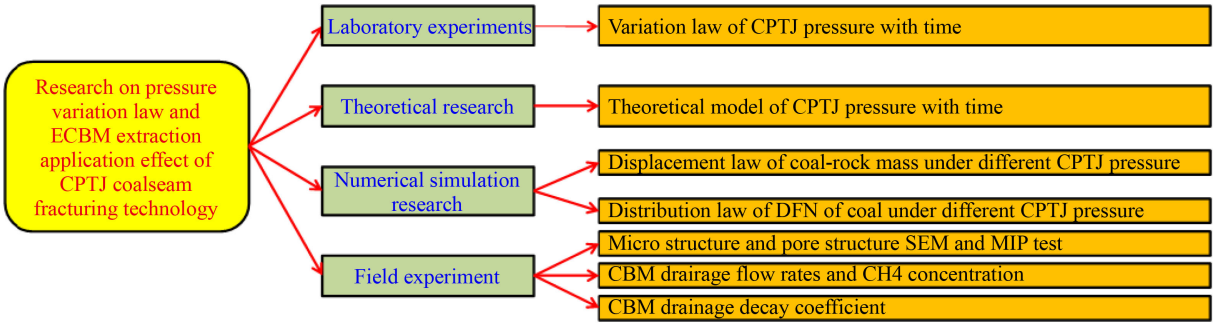

Fig. 3 Research scheme.

2.2.1 Experiment on the pressure change law of CPTJ

Using the CPTJ coal fracturing experimental system shown in Fig. 1, the variation law of CPTJ pressure with time under different initial pressure conditions was studied. In this study, compressed air was used as the power to pressurize the CO_2 in the cylinder and store it in an L-CO_2 storage tank until the pressure in the container reached the set pressure. In this experiment, the target pressure of the L-CO_2 storage tank was set as 10, 20, 30, 40 and 50 MPa. When the pressure of the L-CO_2 storage tank reached the set pressure, the pneumatic valve was opened, and the high-pressure L-CO_2 transiently expanded, forming a high-pressure CO_2 gas jet. The pressure sensor at the jet nozzle was used to measure the fluid pressure change with time.

2.2.2 Numerical simulation of coal damage laws under different CPTJ pressures

A particle-flow code (PFC 2D) is an effective tool to simulate the deformability and crack generation of materials because their basic compositions are bonded particles (He et al., 2021). In this research, the PFC 2D analysis method was used to research the failure law of coal under different CPTJ pressures. As shown in Fig. 4,

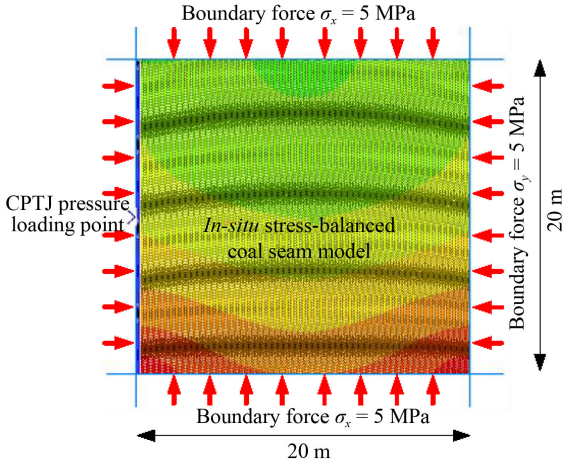

Fig. 4 Schematic diagram of a numerical simulation mode.

a numerical model with a size of 20 m × 20 m was established. The model contained 47546 ball cells with radii of 3–8 mm in a discrete distribution. Assuming that the coal-rock mass model was an infinite medium, viscous boundary conditions for the model were selected, and the reflection of the CPTJ pressure at the infinite boundary of the model was ignored to reduce the calculation. The stress loading of the numerical simulation model mainly included two processes: *in situ* stress static loading and CPTJ dynamic pressure loading, where the latter was the main reason for the destruction of the coal rock mass. In the CPTJ pressure loading stage, an impact point with a diameter of 1.6 cm was set in the center of the left side of the model wall, and then the dynamic CPTJ pressure was applied to the loaded particles.

In the process of model parameter determination and optimization, the uniaxial compression test was used for coal samples (ϕ50 × 100 mm) collected from the mining area, and the results were used to optimize the parameters of the numerical simulation model. Figure 5 shows the experimental and numerical simulation results of coal specimens under uniaxial compression conditions. The results showed that the numerical model results were basically close to the experimental results. Table 1 shows the microscopic parameters of the model after optimization. In the numerical simulation research, the horizontal principal stress and vertical principal stress of the model were both set to 5 MPa, and the displacement of the coal model and the distribution of the discrete fracture network were studied when the jet pressure was $P(t)$, $0.8P(t)$, $0.6P(t)$ and $0.4P(t)$. Among them, $P(t)$ is the CPTJ pressure decay equation with time calculated according to the equipment parameters and the following theoretical research results.

2.2.3 Field test research on CPTJ fracturing to enhance coalbed methane recovery

To study the application effect of CPTJ fracturing technology in enhanced coalbed methane recovery (ECBM), a field experiment was carried out at the S3012 working face of the Shamushu Mine in Sichuan Province using the technology equipment shown in Fig. 2. The

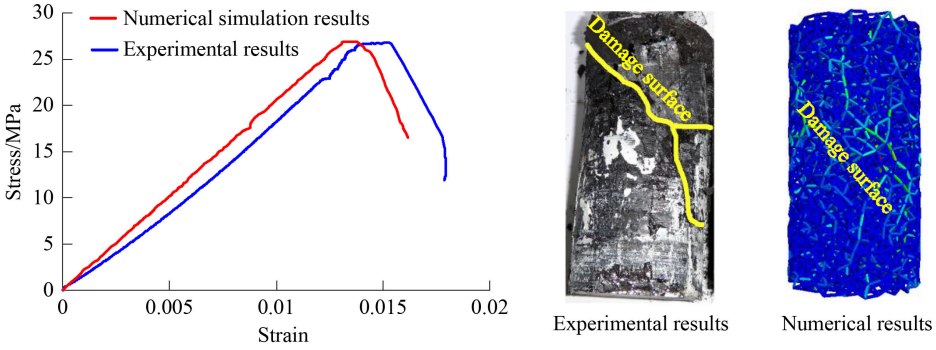

(a) Stress-strain curve (b) Failure mode

Fig. 5 Comparison of experimental and numerical results.

Table 1 Parameters of the PFC model

Parameters	Values	Parameters	Values
Particle diameter ratio	1.1	Cohesion strength of parallel-bond, (Pa)	$13e^6$
Particle density, ρ (kg/m^3)	2500	Friction angle of parallel-bond, (°)	21
Normal critical damping ratio	0.5	Parallel bond radius multiplier, λ	0.8
Stiffness ratio, K_n/K_s	1.3	Contact modulus of particle, E_c (GPa)	1.4
Particle stiffness ratio	1.3	Effective modulus of the parallel bond, $\overline{E}_c$ (GPa)	1.4
Particle friction coefficient, u	0.3	Ratio of normal to shear stiffness of the parallel bond, $\overline{k}_n/\overline{k}_s$	1.3

study area was located in a series of high and steep structural zones (as shown in Fig. 6), with burial depths of 400–520 m, belonging to coal and gas outburst coal mines. Industrial analysis of the coal samples was carried out, and the moisture, ash, volatile matter, and fixed-carbon contents were obtained for the coal samples, as listed in Table 2. Mechanical analysis showed that the uniaxial compressive strength of coal rock was 26.6 MPa, and Poisson's ratio was 0.10–0.14. Field measurements showed that the permeability of coal was 0.0115 m^2/(MPa^2·d), and the methane pressure and methane content of the coal seam were 2.34 MPa and 17.34m^3/t, respectively. Therefore, it was difficult to extract the CBM from the S3012 working face, and it was necessary to use CPTJ fracturing technology to improve the permeability of the coalbed.

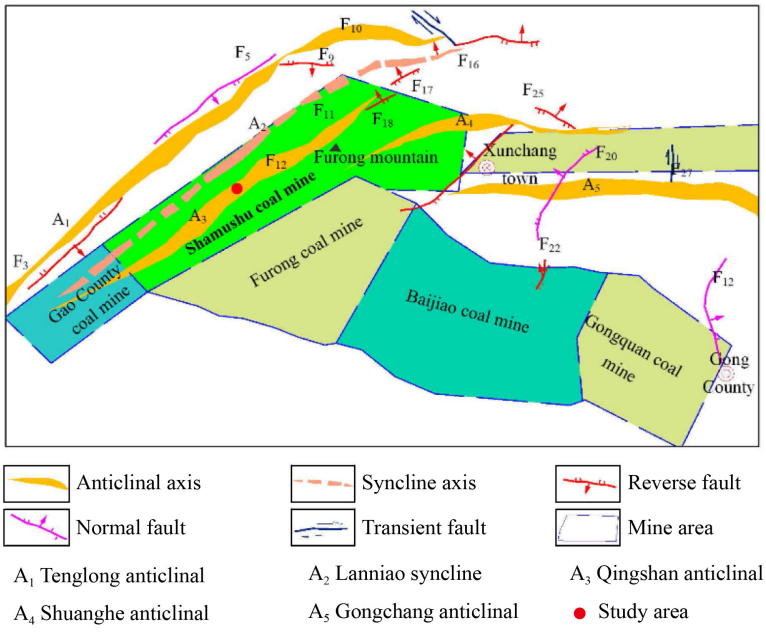

Fig. 6 Geological structure of the study area.

Table 2 Industrial analysis results of the coal samples

Sample	Industrial analysis ($\frac{\text{Maximum value} - \text{Minimum value}}{\text{Average value (Number of samples)}}$)				Coal rank
	Moisture/%	Ash/%	Volatile matter/%	Fixed carbon/%	
#1	0.34	26.67	18.71	54.28	High metamorphic anthracite
#2	0.35	26.50	18.81	53.96	

The field test steps were as follows. First, the experimental borehole shown in Fig. 7 was constructed, and the raw coal samples before CPTJ fracturing were collected. Then, coal seam gas drainage was carried out, and the gas drainage flow rate and CH_4 concentration parameters were monitored for at least one month. Next, coal seam CPTJ fracturing was performed, and coal samples were collected. Similar to the above steps, coal seam gas drainage was carried out after CPTJ fracturing, and its flow rate and concentration parameters were monitored for at least two months. Finally, the change law of coal seam gas drainage parameters before and after CPTJ fracturing was analyzed, and the microstructure and pore structure change characteristics of coal before and after CPTJ fracturing were analyzed by scanning electron microscopy (SEM) and mercury intrusion porosimetry (MIP).

3 Theoretical model research of CPTJ pressure change

3.1 Mass flow equation of the CPTJ system

The theoretical analysis of CPTJ pressure changes is rather complicated because the density of CO_2 gas changes significantly during the flow. Furthermore, the carbon dioxide gas jet fluid is assumed to be a perfect gas with a constant average specific heat value. To simplify the theoretical analysis process in this study, it was assumed that the gas jet was an adiabatic process, and these conditions implied isentropic flow. Furthermore, the CO_2 gas jet fluid was assumed to be a perfect gas with a constant specific heat average value. According to the research results of previous studies (Peng and Zhou, 2008; Woodward and Mudan, 1991; Arnaldos et al., 1998), the CO_2 jet mass flow equation under different jet flow-rate conditions can be obtained.

When the flow rate is subsonic, the mass loss of the fluid per unit time is

$$Q_{\mathrm{m}} = G_{\mathrm{ef}} pS \sqrt{\frac{\gamma M}{RT_0}\left(\frac{2}{\gamma+1}\right)^{\frac{\gamma+1}{\gamma-1}}}, \tag{1}$$

where Q_{m} is the gas mass flow rate at the nozzle outlet; G_{ef} is the gas expansion factor under subsonic condition $G_{\mathrm{ef}} = \sqrt{\left(\frac{p}{p_0}\right)^{\frac{2}{\gamma}} \cdot \left[1 - \left(\frac{p}{p_0}\right)^{\frac{\gamma-1}{\gamma}}\right] \cdot \left[\left(\frac{2}{\gamma-1}\right) \cdot \left(\frac{\gamma+1}{2}\right)^{\frac{\gamma+1}{\gamma-1}}\right]}$; p is the gas pressure at the nozzle outlet; S is the cross sectional area of the nozzle outlet; γ is the heat capacity ratio, γ = 1.33; R is the molar gas constant, R = 8.314 J/(mol·K); T_0 is the temperature in the nozzle; and p_0 is the gas pressure inside the nozzle.

When the flow rate is sonic or supersonic, the mass loss of the fluid per unit time is

$$Q_{\mathrm{m}} = G_{\mathrm{ef}} pS \sqrt{\frac{\gamma M}{RT_0}\left(\frac{2}{\gamma+1}\right)^{\frac{\gamma+1}{\gamma-1}}} = pS \sqrt{\frac{\gamma M}{RT_0}\left(\frac{2}{\gamma+1}\right)^{\frac{\gamma+1}{\gamma-1}}}, \tag{2}$$

where the gas expansion factor G_{ef} = 1.

Combining Eq. (1) and Eq. (2), the mass loss of the fluid per unit time can be obtained as:

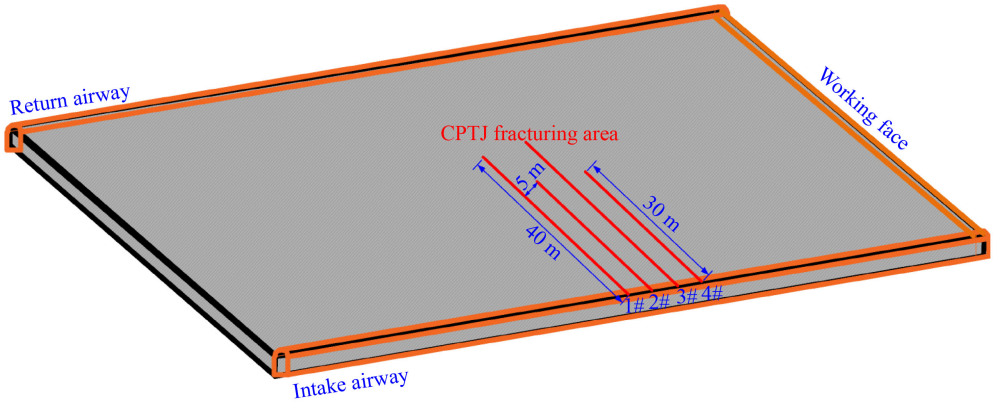

Fig. 7 Layout of field experiment boreholes.

$$Q_{\mathrm{m}} = G_{\mathrm{ef}} pS \sqrt{\frac{\gamma M}{RT_0}\left(\frac{2}{\gamma+1}\right)^{\frac{\gamma+1}{\gamma-1}}} \begin{cases} G_{\mathrm{ef}} = 1, & \text{Subsonic flow} \\ G_{\mathrm{ef}} = \sqrt{\left(\frac{p}{p_0}\right)^{\frac{2}{k}}\left[1-\left(\frac{p}{p_0}\right)^{\frac{k-1}{k}}\right]\left[\left(\frac{2}{k-1}\right)\left(\frac{k+1}{2}\right)^{\frac{k+1}{k-1}}\right]}, & \text{Sonic or supersonic flow} \end{cases} . \tag{3}$$

3.2 Theoretical model of CPTJ pressure

In the process of CPTJ, the flow rate and pressure are continuous parameters that change with time. Ignoring the heat exchange and gravitational influence in the CPTJ process, the main variables that change with time (t) in the system during the gas jet process are CO_2 gas pressure (p), gas flow rate (Q_{m}), and CO_2 gas mass loss (m_1). The following equation is satisfied by the three parameters of m_s, Q_{m} and t:

$$m_1 = \int_0^t Q_{\mathrm{m}} \mathrm{d}t. \tag{4}$$

It is assumed that the CO_2 gas satisfies the ideal gas equation of state before and after the jet. The initial mass of CO_2 in the jet system is m, the remaining mass after m_1 is lost in the jetting process is $m–m_1$, and the volume and pressure are $V\frac{m-m_1}{m}$ and p, respectively. Then, the following equations are satisfied:

$$\begin{cases} p_0 V \frac{m-m_1}{m} = RT_0 \frac{m-m_1}{M} \\ pV = RT_0 \frac{m-m_1}{M} \end{cases} . \tag{5}$$

According to Eq. (3) to Eq. (5), the loss of the CO_2 phase transition jet satisfies the following equations:

$$\begin{cases} Q_{\mathrm{m}} = G_{\mathrm{ef}} pS\left(\frac{\gamma M}{RT_0}\left(\frac{2}{\gamma+1}\right)^{\frac{\gamma+1}{\gamma-1}}\right)^{\frac{1}{2}} \\ p_0 \frac{m-m_1}{m} = p \\ m_1 = \int_0^t Q_m \mathrm{d}t \end{cases} . \tag{6}$$

Let $S\left(\frac{\gamma M}{RT_0}\left(\frac{2}{\gamma+1}\right)^{\frac{\gamma+1}{\gamma-1}}\right)^{\frac{1}{2}} = C$. Then $m_1 = \int_0^t Q_{\mathrm{m}} dt = \int_0^t G_{\mathrm{ef}} \cdot C p_0 \frac{m-m_1}{m} \mathrm{d}t$, and then we can get:

$$\frac{\mathrm{d}m_1}{\mathrm{d}t} + \frac{G_{\mathrm{ef}} C p_0}{m} m_1 = G_{\mathrm{ef}} C p_0. \tag{7}$$

Let $\frac{G_{\mathrm{ef}} C p_0}{\mathrm{m}} = A$, $G_{\mathrm{ef}} C p_0 = B$. Then, from Eq. (7), we can obtain

$$m_1 = De^{-At} + m, \tag{8}$$

where D is a constant determined by the initial conditions of the equation. When $t = 0$, $m_1 = 0$, and $D = –m$ can be obtained. From this, the theoretical equation for the CPTJ pressure decay with time is obtained as follows:

$$\begin{cases} m_1 = m\left(1-e^{-At}\right) \\ Q_{\mathrm{m}} = \frac{\mathrm{d}m_1}{\mathrm{d}t} = \mathrm{m}Ae^{-At} \\ p = p_0 \frac{m-m_1}{m} = p_0 e^{-At} \end{cases} . \tag{9}$$

According to Eq. (9), combined with the parameters of the CPTJ coal fracturing ECBM technology equipment, when the CO_2 filling weight is 2.7 kg and the rupture disc threshold pressure is 276 MPa, the change in the CPTJ pressure with time satisfies the equation $P(t) = 276e^{-19.92t}$.

4 Results analysis

4.1 Variation law of CPTJ pressure with time

In the experimental research, a gas pressure sensor was used to measure the variation in the CO_2 gas jet pressure. Figure 8 shows the pressure change curve of the CPTJ with time under storage tank pressures of 10, 20, 30, 40, and 50 MPa. Figure 8 clearly shows that the jet pressure in the CPTJ process decreased rapidly with time and showed an exponential development trend under different initial pressure conditions. An exponential equation was used to fit the CPTJ pressure curve with time, and the fitting equation and the corresponding determination coefficient (i.e., R^2) under different initial pressure conditions are shown in Table 3.

4.2 Numerical simulation results

Under the action of CPTJ fracturing technology, coal rock masses are damaged, a certain displacement occurs, and a discrete fracture network (DFN) is generated. It is important to study the displacement and distribution of DFNs to research the permeability enhancement effect of CPTJ fracturing on coal seams.

Figure 9, which was produced using numerical simulation, shows the displacement cloud diagram of the coal-rock mass damaged by the CPTJ at various pressures. The deformation of the coal-rock mass mainly occurred near the point of action of the CPTJ, and the particles of the coal-rock produced reverse displacement under the action of the CPTJ. The displacement of the coal body decreased with decreasing CPTJ pressure. The maximum displacement of the coal body was 6.79 m when the jet pressure was $P(t)$. When the CPTJ pressure decreased by 20%, its displacement decreased to 3.39 m, 3.65 m, and 2.71 m.

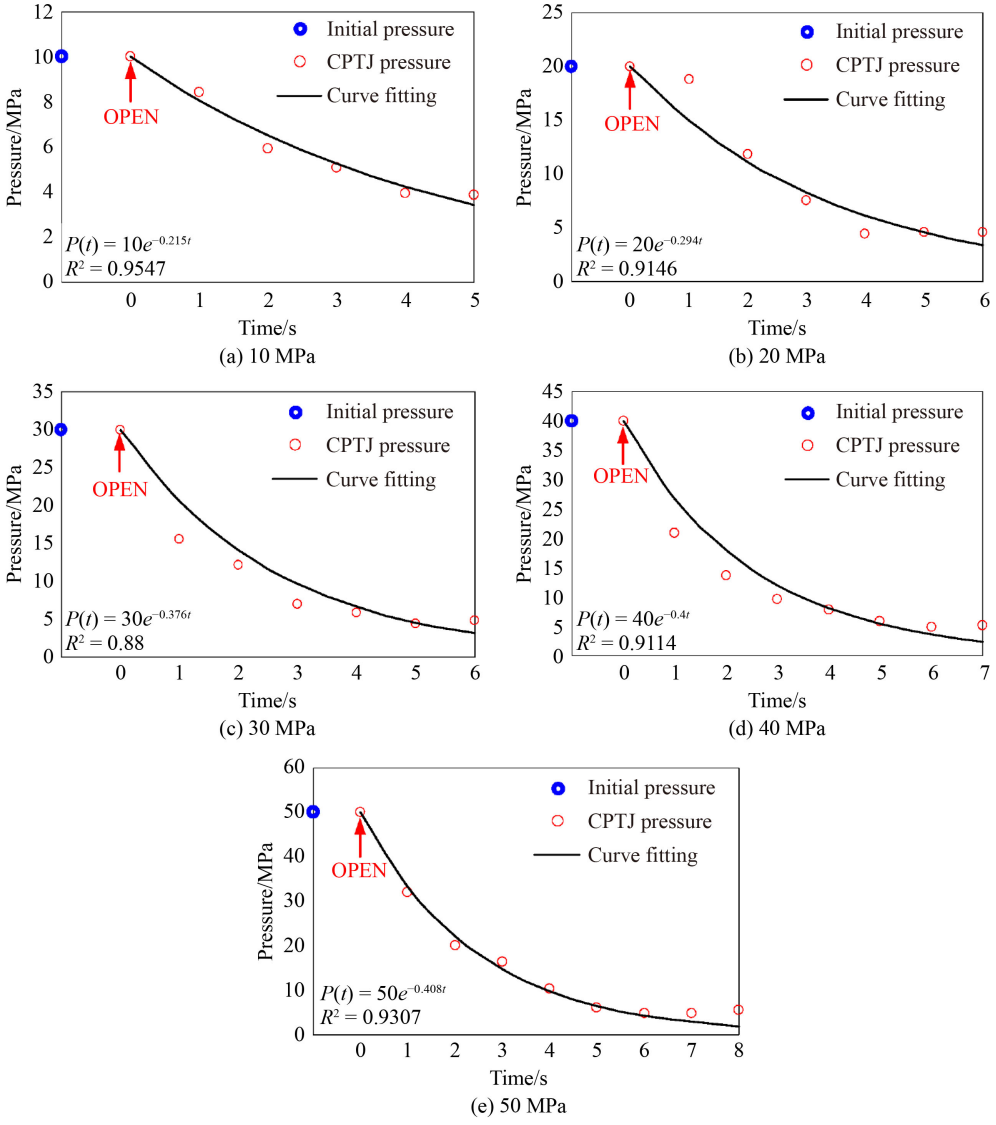

Fig. 8 Law of CPTJ pressure changing with time under different initial pressures and its exponential fitting curve.

Table 3 Fitting equation of CPTJ pressure changing with time under different initial pressures

Initial pressure P_0/MPa	Fitted curve equation	Fitting parameter m	R^2
10	$P(t) = P_0e^{-mt}$	0.215	0.96
20		0.294	0.92
30		0.376	0.88
40		0.400	0.91
50		0.408	0.93

According to the results of the numerical simulation, Fig. 10 shows the DFN distribution of coal after CPTJ fracture under different pressures. The figure shows that the unit number of DFN fractures of the coal body after fracturing decreased with decreasing CPTJ pressure. When the jet pressure $P(t)$ decreased by 20% in turn, the number of DFN fracture units decreased from 27860 to 19238, 18584 and 9643. Furthermore, with the decrease in jet pressure, the horizontal expansion size of the discrete fracture network decreased significantly.

4.3 SEM test results

In this paper, the microscopic pore and fracture structures of coal rock before and after CPTJ fracturing were tested by using scanning electron microscopy (SEM). The test results are shown in Fig. 11.

The SEM results indicated that the coal samples had different distribution characteristics of microscopic pores and fractures. For the raw coal samples (Fig. 11(a)), independent and unconnected microscopic pores and microcracks were clearly shown on the coal surface, and the surface was smooth with almost no broken particles. This microstructural feature led to the coal seam having good methane storage capacity but low permeability, which was not conducive to the drainage of CBM. After conducting CPTJ fracturing, the surface morphologies of

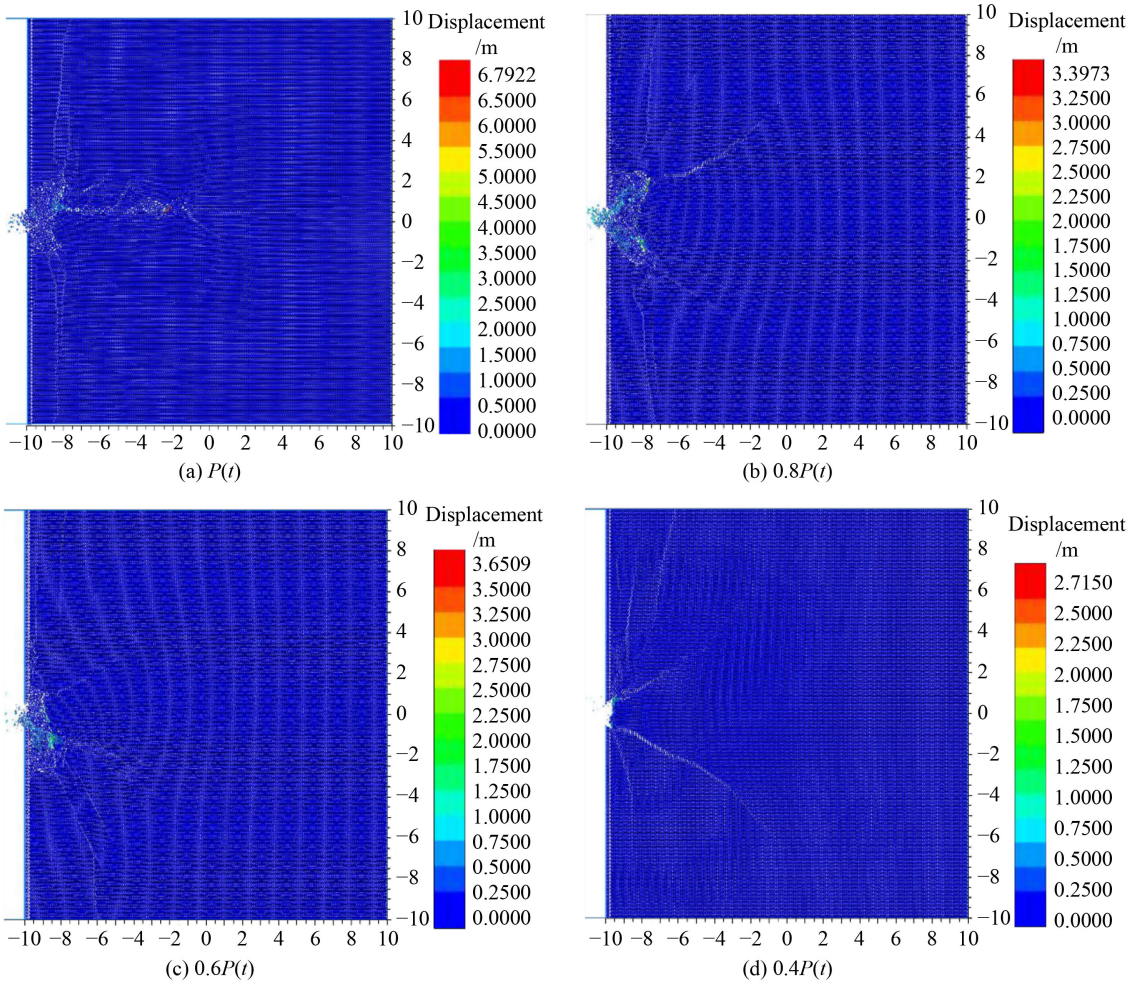

Fig. 9 Displacement cloud diagram of coal-rock mass damaged by CPTJ at different pressures.

coal samples were altered, as shown in Figs. 11(b)–11(e), which show the SEM test results of the surface morphologies of the #1–#4 drilled coal samples, respectively. It can be seen from the SEM image that a series of fractured cracks and broken particles with irregular shapes were produced on the coal samples after CPTJ fracturing. Furthermore, the pore size and depth of the coal samples after fracturing were much larger than those of the original coal samples, and these pores had various shapes, such as oval, circular, and slit shapes. Some of these pores and fractures were connected with each other due to the shock and fracture effects caused by CPTJ. These interconnected fractures could act as channels for gas flow. Since the increase in interconnected pores and cracks in coalbeds can effectively enhance the gas permeability of CBM reservoirs (Yan et al., 2020), CPTJ fracturing technology is an effective method for ECBM of low-permeability coal seams.

4.4 MIP test results

Coal rock is a typical porous medium reservoir, and its pore space is of great significance for gas storage. Therefore, it is essential to accurately describe the pore structure of coal rock masses to determine their permeability (Zhao et al., 2022). The MIP method was used to investigate the application effect of CPTJ fracturing in enhancing the pore structure of coal, such as porosity, pore size distribution, and specific surface area. According to the test results, the total pore volume and porosity of the coal samples were obtained. Furthermore, the Hodot classification method of pore size was used to classify the pore characteristics of coal samples as follows (Hodot, 1966): micropores (< 0.01 μm), transition pores (0.01–0.1 μm), mesopores (0.1–1 μm), and macropores (> 1 μm), as shown in Table 4. The pore size distributions and cumulative pore volumes of the raw coal samples and coal subjected to CPTJ are shown in Figs. 12 and 13.

Table 4 shows that under the effect of CPTJ, the pore capacity of various types of coal pores increased to varying degrees. After CPTJ fracturing, the total pore volume of the coal seam was 2.31–3.03 times that of the raw coal seam, and the average pore capacities of the micropores, transition pores, mesopores, and macropores were 1.03, 3.34, 2.54, and 3.82 times that of the raw coal

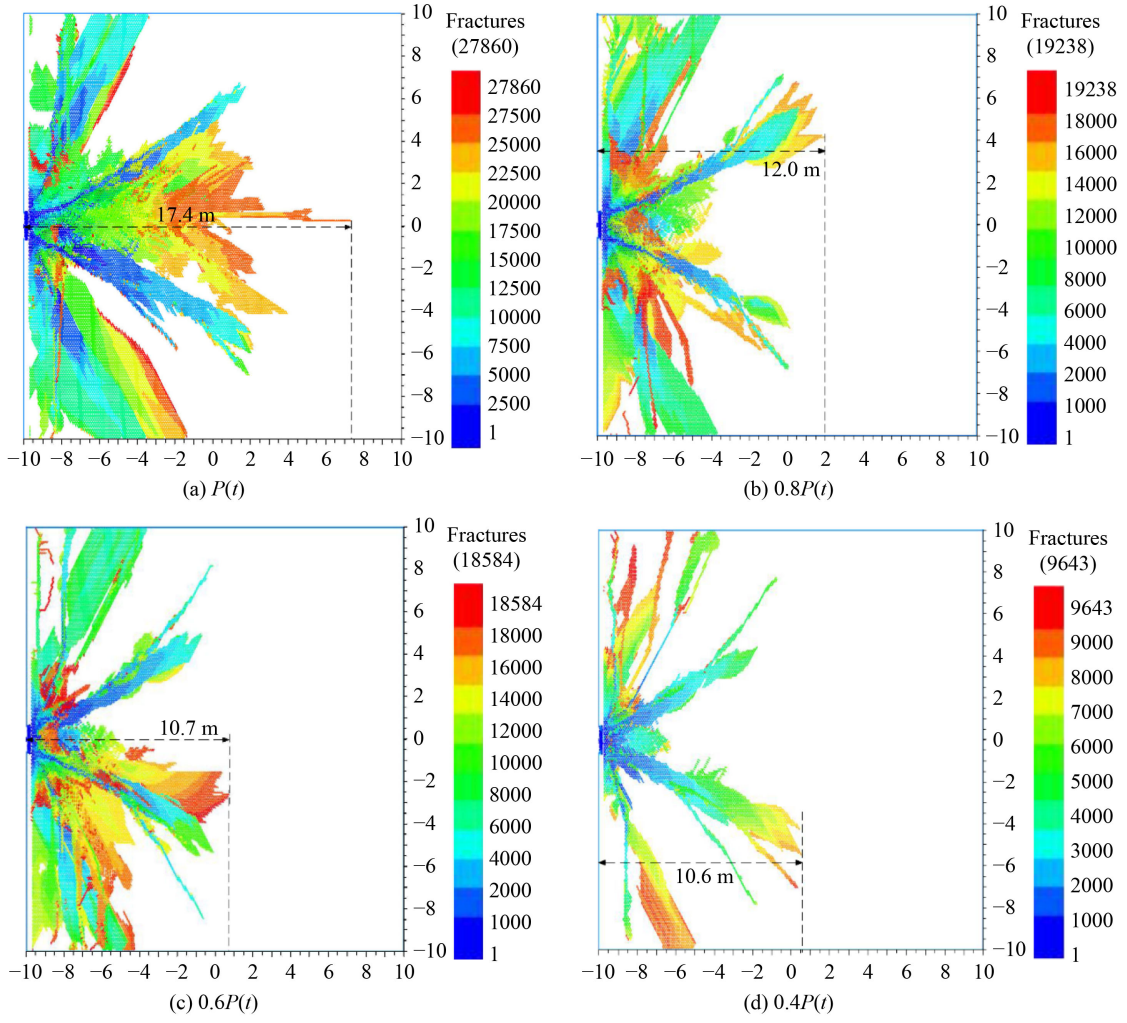

Fig. 10 Distribution characteristics of the DFN under different CPTJ pressures.

seam, respectively. According to the analysis, CPTJ fracturing can significantly increase the number of transition pores and macropores in coal seams. The increase in macropore pore capacity is conducive to the seepage of coalbed methane.

The volume of macropores and cumulative pore volume in coal samples after CPTJ fracturing significantly increased compared with raw coal samples, as shown in Figs. 12 and 13. The above phenomena can be explained as follows. A large amount of high-pressure gas was injected into the coal body during the CPTJ fracturing process, which caused the coal to fracture under the action of impact stress and CO_2 phase transition expansion. While many pores formed, some primary micropores and mesopores developed into macropores. This further resulted in the specific surface area of the coal body after CPTJ fracturing being significantly less than that of raw coal, as shown in Table 4. The capacity of coal to adsorb methane decreased with the decrease in specific surface area, which improved the desorption of methane. Simultaneously, the porosity of coal after CPTJ fracturing was 2.47 to 2.76 times greater than that of the raw coal seam, which improved the connectivity of the coal's pores. In summary, the research results of the MIP analysis indicate that CPTJ fracturing technology can efficiently increase the pore structure and permeability of coal, which will be effective for the efficient drainage of coalbed methane.

4.5 Field test results

Coalbed methane drainage flow rates and methane concentration are important indicators of recovery efficiency. The change curve of the CBM drainage flow rate of test boreholes #1 to #4 before and after CPTJ fracturing was achieved, as shown in Fig. 14, based on the monitoring data from the field test.

It is obvious that after CPTJ fracturing, the variation in CBM extraction flow rates over time showed a strong upward trend, and the four experimental boreholes increased by 520%, 760%, 780%, and 980%, respectively, indicating that the gas drainage efficiency was effectively improved. The repeatable results of the four different groups are shown in Figs. 14 (a)–14(d). During

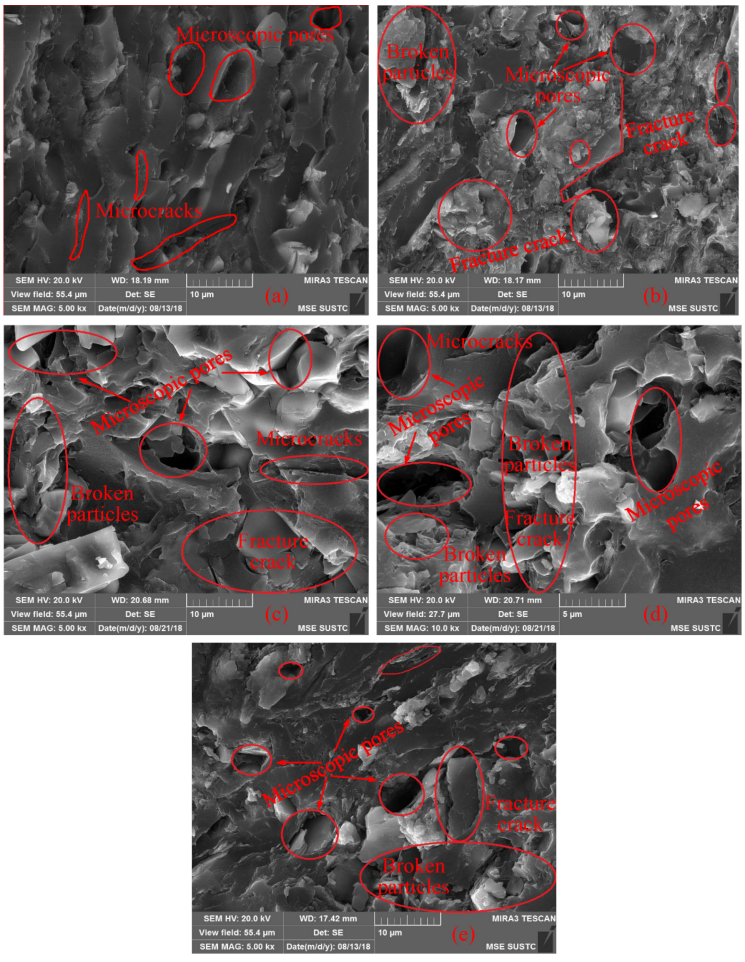

Fig. 11 SEM results. (a) Raw coal sample; (b) #1 borehole; (c) #2 borehole; (d) #3 borehole; and (e) #4 borehole.

Table 4 Pore structure parameters of coal samples

Samples No.	Pore volume/($mm^3 \cdot g^{-1}$)				Total pore volume/($mm^3 \cdot g^{-1}$)	Specific surface area/($m^2 \cdot g^{-1}$)	Porosity/%
	Micro-	Transition	Meso-	Macro-			
A	18.1	5.1	6.5	26.8	56.5	18.73	9.12
B	22.2	18.7	17.6	106.7	165.2	14.55	24.5
C	17.4	20.4	19.8	113.6	171.2	14.75	25.2
D	15.8	12.9	13.2	88.6	130.5	16.21	22.6
E	19.3	16.2	15.5	100.6	151.6	15.72	24.8

Notes: A is raw coal sample; B, C, D and E are the coal samples after CPTJ fracturing of 1 #, 2 #, 3 # and 4 # boreholes respectively.

the extraction process, low methane concentrations and small quantities of pure gas are the main causes of low permeability coal seam gas drainage that does not meet production requirements. Another significant effect supplied by CPTJ fracturing technology is that it can enhance the concentration of gas drainage. The research results showed that after fracturing, it increased by 140%–210% when compared to the raw coal seam. Therefore, CPTJ fracturing technology can achieve significant improvements in gas drainage. Table 5 gives some values to demonstrate this capability of the CPTJ fracturing technology.

5 Discussion

5.1 Theoretical model verification

To prove the correctness of the theoretical model developed in Section 3, the experimental research results in Section 4.1 were used for verification. From Section 2.1.1, we obtained that the volume of the high-pressure L-CO_2 storage tank of the experimental system was 5 L, the cross-sectional area (S) of the nozzle was 4.91 mm^2, and the molar mass (M) of CO_2 was 44 g/mol. According to the above parameters, the constant $C = 1.37 \times 10^{-8}$ in Eq. (7) was calculated. When the initial pressure of CO_2 was

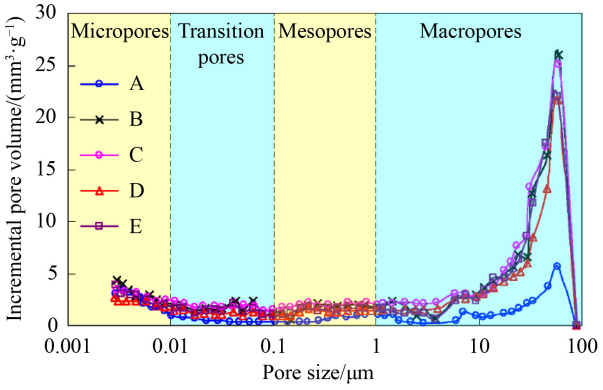

Fig. 12 Pore size distributions of coal samples.

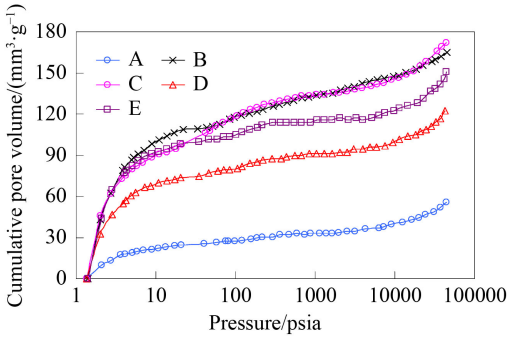

Fig. 13 Cumulative pore volumes of coal samples.

10 MPa, $m = 2.8$ kg, $G_{ef} = 4.22$, and the constant $A = 0.206$ in Eq. (9) was calculated. Then, when the initial pressure of CO_2 was 10 MPa, the variation law of CO_2 phase transition jet pressure with time conformed to the following equation:

$$p = p_0 e^{-At} = 10e^{-0.206t}. \quad (10)$$

In the same way, when the initial pressure of CO_2 was 20, 30, 40, and 50 MPa, the theoretical equations of the CO_2 phase transition jet pressure change with time was obtained as shown in Table 6. Comparing the fitting equation of the experimental data in Table 3 with the theoretical equation in Table 6, the deviation rate of parameter A was obtained.

According to Table 6, the maximum deviation between the theoretical equation and the fitting parameters of the liquid CO_2 phase change jet pressure change with time was 8.82%, the minimum value was 2.41%, and the average value was 5.61%. The pressure of the CPTJ followed an exponential relationship with time, and the established theoretical equation was consistent with the time change in the pressure of the CO_2 phase transition jet.

5.2 Influence of pressure on CPTJ fractured coal

According to Fig. 9, the change curve of the maximum displacement of the coal-rock mass with the CPTJ pressure was obtained, as shown in Fig. 15. Under the action of CPTJ, as the pressure decreased, the displacement of the coal-rock mass gradually decreased. According to Fig. 10, the relationship between the number of DFN fracture units and the expansion size and the CPTJ pressure was obtained, as shown in Fig. 16.

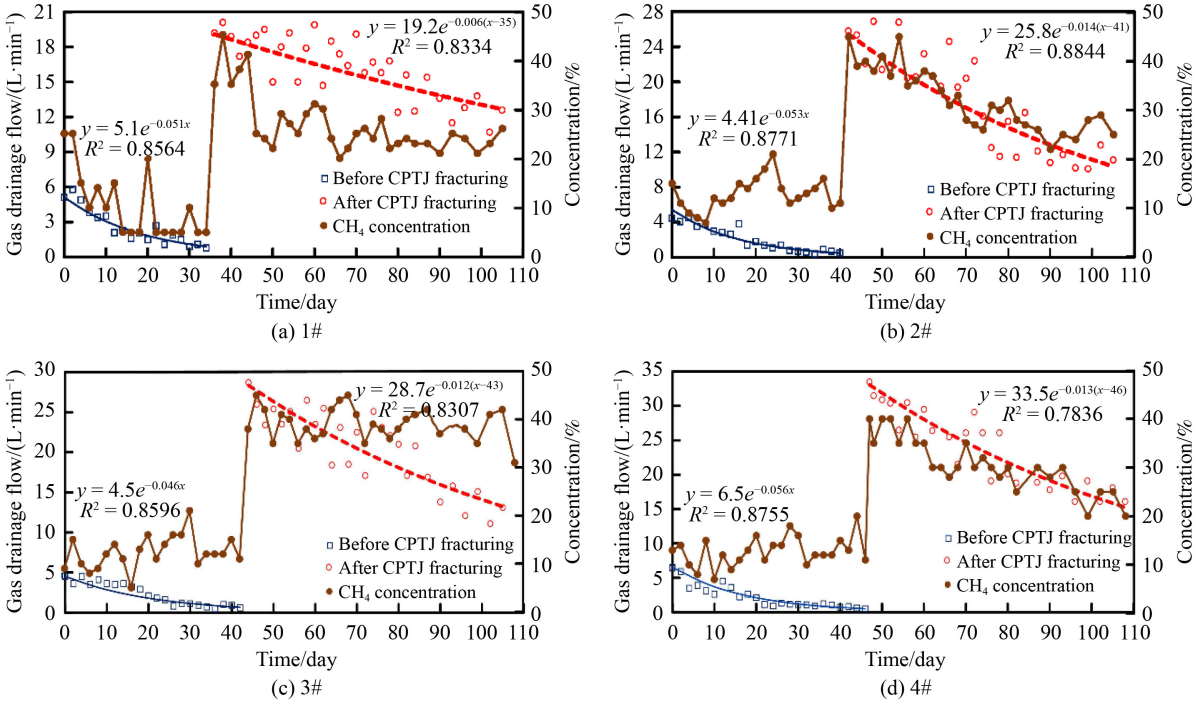

Fig. 14 Variation in CBM drainage flow rates of experimental boreholes.

Table 5 Specific parameters of CPTJ technology to enhance CBM recovery

Boreholes No.		1#	2#	3#	4#
Average gas drainage flow rates/(L·min^{-1})	Raw coal seam	2.6	2.1	2.3	2.2
	After CPTJ fracturing	16.2	18.0	20.2	23.7
Increase percentage/%		520%	760%	780%	980%
Average concentration/%	Raw coal seam	10.5	12.9	12.4	12.8
	After CPTJ fracturing	26.8	32.3	39	30.8
Increase percentage/%		160%	150%	210%	140%

Table 6 Theoretical equation of CPTJ pressure variation with time and its parameter comparison with the experimental fitting equation

Initial pressure P_0/MPa	Theoretical equations	Experimental fitting equations	Deviation rate/%
10	$p = 10e^{-0.206t}$	$p = 10e^{-0.215t}$	4.23
20	$p = 20e^{-0.287t}$	$p = 20e^{-0.294t}$	2.41
30	$p = 30e^{-0.343t}$	$p = 30e^{-0.376t}$	8.82
40	$p = 40e^{-0.366t}$	$p = 40e^{-0.400t}$	8.58
50	$p = 50e^{-0.424t}$	$p = 50e^{-0.408t}$	4.03

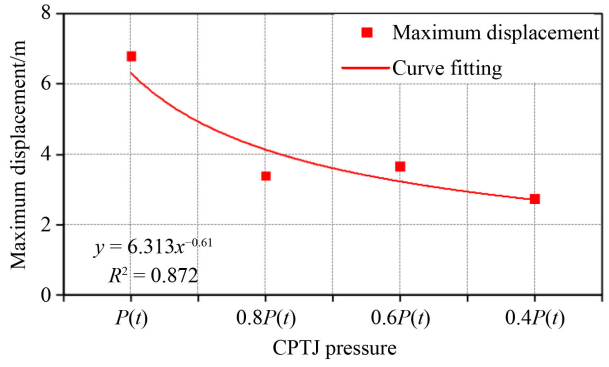

Fig. 15 Variation curve of the maximum displacement of coal rock and CPTJ pressure.

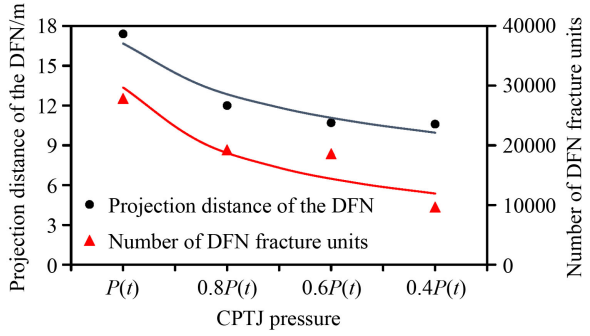

Fig. 16 Relationship between the DFN fracture units, the projection distance of the DFN fractures in the horizontal direction and CPTJ pressures.

With the decrease in CPTJ pressure, the number of DFN fracture units in coal decreased, and the projection distance of fractures in the horizontal direction decreased significantly.

The results implied that the displacement, number of discrete fracture network units and the expansion size of the CBM reservoir caused by CPTJ damage decreased as the jet pressure decreased because the force exerted on the CBM reservoir decreased with decreasing jet pressure. Furthermore, the larger the damage displacement formed on the CBM reservoir was, the greater the degree of CBM reservoir breakage, the more cracks formed on the coal seam, and the more favorable the coalbed gas seepage. Therefore, within a safe range, increasing the CPTJ pressure is beneficial to increasing the coal seam gas permeability.

5.3 Influence of CPTJ fracturing on the decay law of CBM drainage

In many cases of CBM drainage practice, rapidly falling gas extraction flow rate measurements are frequently observed in gas extraction operations, especially in low permeability CBM reservoirs (Karacan et al., 2011; Liu and Cheng, 2014). That is, the gas drainage flow rate and concentration drop rapidly after the coal seam borehole starts gas drainage, which not only brings difficulties to CBM drainage but also brings many safety hazards to coal mining. Therefore, the national mine safety administration of China uses the coal seam gas drainage flow rate decay coefficient as an important indicator to assess the difficulty of coal seam gas drainage, as shown in Table 7. The attenuation coefficient of CBM drainage flow rates is a characteristic coefficient of the CBM flow rates of the borehole in coal seams decaying with time, which is obtained by fitting the data collected from the field test. The fitting equation is $q_t = q_0 e^{-\beta t}$, where β is the gas drainage attenuation coefficient, t is the gas drainage time, q_0 is the initial gas drainage flow rate, and q_t is the gas drainage flow rate after t days (Yu and Cheng, 2012).

According to the variation trend of the CBM drainage

Table 7 Corresponding relationship between the decay coefficient and difficulty level of CBM drainage

Decay coefficient	<0.003	0.003–0.05	>0.05
Difficulty level of CBM drainage	Easily	Barely	Difficulty

flow rates with time (Fig. 14), the exponential fitting method was used to obtain the attenuation coefficient of the gas drainage flow, as shown in Fig. 17. Figure 17 shows that before CPTJ fracturing, the attenuation coefficients of boreholes #1, #2, #3, and #4 were 0.051, 0.053, 0.046 and 0.056, respectively. All these parameters were almost greater than 0.05. According to Table 7, it was difficult to extract gas from the experimental area. After CPTJ fracturing, the attenuation coefficients were 0.006, 0.014, 0.012 and 0.013, which were 88.24%, 73.58%, 73.91% and 76.79% less than those before fracturing, respectively. All these parameters were less than 0.05 and greater than 0.003. This shows that CPTJ technology can effectively reduce the difficulty level of coal seam gas drainage and reduce the difficulty of CBM drainage from coal seams.

5.4 Mechanism of CPTJ fracturing to ECBM

Coal is a heterogeneous material that is composed of a fracture network and matrix, and the main passage for gas flow is contained in fractures (Sampath et al., 2021; Li et al., 2021). Under natural conditions, the pores and fractures of coal seams are closed under the effect of *in situ* stress (Liu et al., 2018; Lu et al., 2020), with low permeability and few gas migration channels (Wang et al., 2021), resulting in difficult gas drainage, as shown in Fig. 18 (a).

Through CPTJ fracturing, low permeability coal seams are damaged and fractured under the force of a high-pressure CO_2 gas jet. Under the continuous action of *in situ* stress, these fractures continue to expand. This forms a pressure relief fracture field around the fracturing hole, increases the number of connected pores in the coal body, establishes a channel for gas migration, and enhances the coal seam permeability (Cao et al., 2022; Liao et al., 2021; Cheng et al., 2020). At the same time, the fractures constructed by CPTJ technology cause the stress in the coal seam to redistribute, forming a localized area of pressure relief. This prompts the raw closed fractures in the coal body to reopen, reducing the effective stress on the coal body and destroying the dynamic balance of CH_4 adsorption and desorption in the coal seam, which results in desorption of CH_4 (Cheng et al., 2021b). Under the influence of the pressure difference, free CH_4 migrates to the coal seam fissure, increasing the flow and concentration of CBM drainage. Furthermore, since the coal seam has a stronger capacity for adsorption of CO_2 than CH_4, after CO_2 gas enters the fracture, competitive adsorption promotes the desorption of CH_4 (Du et al., 2021), which can further improve the CH_4 concentration of coal seam gas and decrease the attenuation of flow, as shown in Fig. 18 (b).

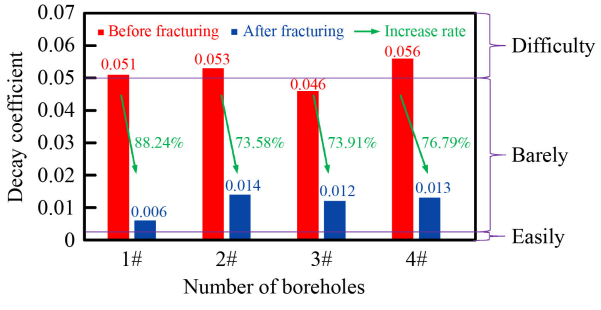

Fig. 17 Change law of the gas drainage flow rate decay coefficient after CPTJ fracturing.

6 Conclusions

In this paper, to obtain the pressure variation law of CPTJ fracturing technology, the influence of its jet pressure on cracked coal rock was revealed, and its enhanced CBM extraction effect was clarified. A series of laboratory experiments, theoretical studies, numerical simulations and field experiments were carried out. Based on the above research and analysis, the following important conclusions were obtained.

1) Experimental studies showed that the CPTJ pressure decayed exponentially with time. Theoretical research established an exponential equation of CPTJ pressure variation with time. After verification, the average deviation between the theoretical calculation parameters and the fitting parameters was 5.61%.

2) The numerical simulation study of CPTJ coal rock fracturing under different jet pressure conditions was carried out by the PFC method, and the relationship between the coal rock damage displacement, the distribution of DFN and the jet pressure was obtained. The research results showed that with decreasing jet pressure, the failure displacement of coal, the number of fracture units and their extension sizes gradually decreased. The CPTJ pressure mainly affected the number and expansion size of coal rock breaking fractures but did not affect the development direction of fractures.

3) Field tests showed that, compared with the raw coal seam, CPTJ could effectively increase the number of connectable macropores and fractures in coal seams, strongly increase the CBM drainage flow rate by between 5.2 times and 9.8 times, and significantly reduce the CBM drainage decay coefficient by between 73.58% and 88.24%.

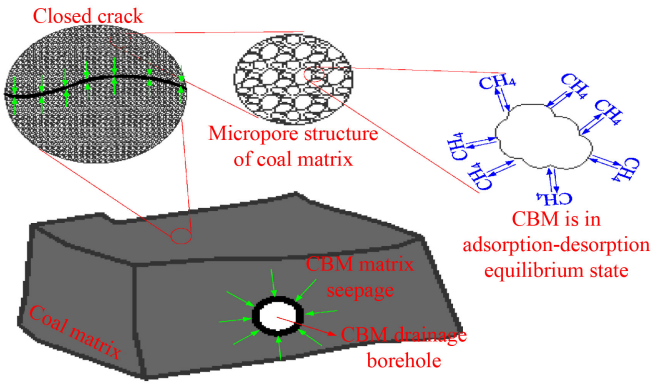

(a) Schematic diagram of gas drainage from a raw coal seam

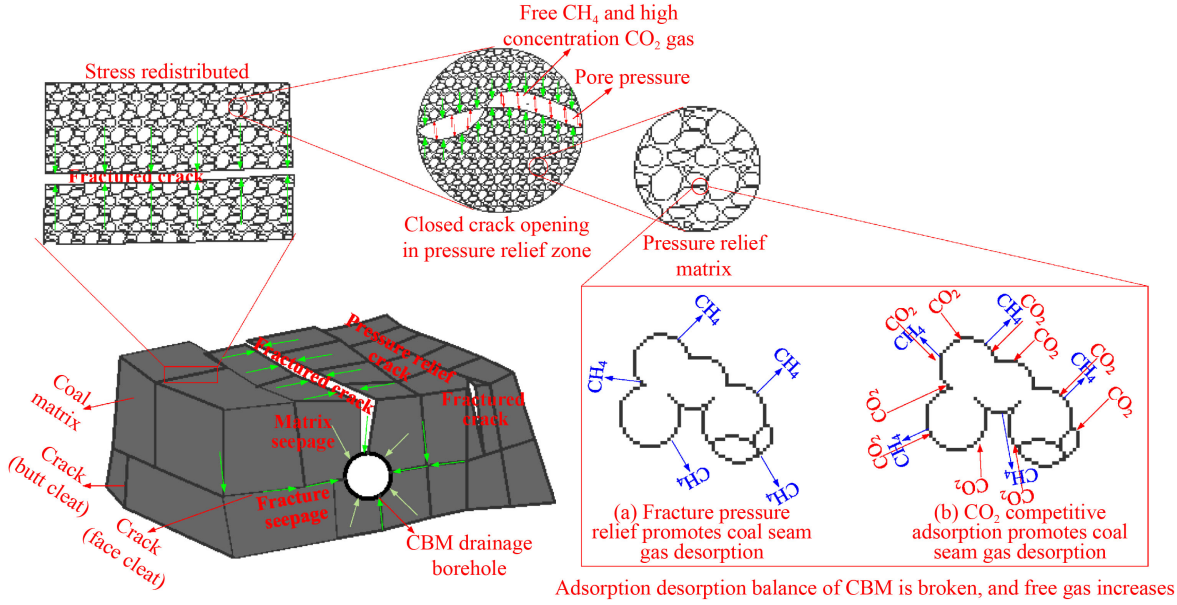

(b) Schematic diagram of gas drainage in coal seams after CPTJ fracturing

Fig. 18 Schematic diagram of gas drainage before and after CPTJ fracturing.

Acknowledgments This research was partially supported by the National Natural Science Foundation of China (Grant Nos. 52204095, 51974163, 52274127 and 52174174), the National Key Research and Development Program of China (No. 2021YFC2902104), the Natural Science Foundation of Hunan Province, China (No. 2023JJ30509), the Key Laboratory of Safety and High-efficiency Coal Mining of Ministry of Education (No. JYBSYS2020204), the Special Program for Basic Research of Key Scientific Research Projects of Colleges and Universities in Henan Province of China (No. 21ZX004), and the Innovative Scientific Research Team of Henan Polytechnic University in China (No. T2022-1).

References

Ainalis D, Kaufmann O, Tshibangu J P, Verlinden O, Kouroussis G (2017). Modelling the source of blasting for the numerical simulation of blast-induced ground vibrations: a review. Rock Mech Rock Eng, 50(1): 171–193

Arnaldos J, Casal J, Montiel H, Sánchez-Carricondo M, Vílchez J A (1998). Design of a computer tool for the evaluation of the consequences of accidental natural gas releases in distribution pipes. J Loss Prev Process Ind, 11(2): 135–148

Bai X, Zhang D, Zeng S, Zhang S, Wang D, Wang F (2020). An enhanced coalbed methane recovery technique based on CO_2 phase transition jet coal-breaking behavior. Fuel, 265(4): 1–11

Barnhart E, Weeks E, Jones E, Ritter D, Mcintosh J, Clark A, Ruppert L, Cunningham A, Vinson D, Orem W (2016). Hydrogeochemistry and coal-associated bacterial populations from a methanogenic coal bed. Intern J Coal Geo, 162(5): 14–26

Byrer C, Havryluk I, Uhrin D (2014). Chapter 1– Coalbed Methane: A Miner's Curse and a Valuable Resource. Amsterdam: Elsevier Inc

Cao Y X, Zhang J, Zhai H, Fu G, Tian L, Liu S M (2017). CO_2 gas fracturing: a novel reservoir simulation technology in low permeability gassy coal seams. Fuel, 203: 197–207

Cao Y X, Zhang J, Zhang X, Liu S, Derek E (2022). Micro-fractures in coal induced by high pressure CO_2 gas fracturing. Fuel, 311: 1–10

Chen H D, Wang Z F, Chen X, Chen X, Wang L (2017). Increasing permeability of coal seams using the phase energy of liquid carbon dioxide. J CO_2 Util, 19: 112–119

Cheng L, Li D, Wang W, Liu J (2021a). Heterogeneous transport of

free CH_4 and free CO_2 in dual-porosity media controlled by anisotropic *in situ* stress during shale gas production by CO_2 flooding: implications for CO_2 geological storage and utilization. ACS Omega, 6(40): 26756–26765

Cheng L, Zhang Y, Liu J, Lu Z, Zeng C, Zhao P (2021b). Numerical modeling of the dynamic variation in multiphase CH_4 during CO_2 enhanced gas recovery from depleted shale reservoirs. Front Earth Sci, 15(4): 790–802

Cheng Y, Zeng M, Lu Z, Du X, Yin H, Yang L (2020). Effects of supercritical CO_2 treatment temperatures on mineral composition, pore structure and functional groups of shales: implications for CO_2 sequestration. Sustainability, 12(9): 1–22

Deng B, Yin G, Zhang D, Li M, Liu Y, Lu J (2018). Experimental investigation of fracture propagation induced by carbon dioxide and water in coal seam reservoirs. Powder Technol, 338(10): 847–856

Dowding C H, Hamdi E, Aimone-Martin C T (2016). Strains induced in urban structures by ultra-high frequency blasting rock motions: a case study. Rock Mech Rock Eng, 49(10): 4073–4090

Du X, Cheng Y, Liu Z, Yin H, Wu T, Huo L, Shu C (2021). CO_2 and CH_4 adsorption on different rank coals: a thermodynamics study of surface potential, Gibbs free energy change and entropy loss. Fuel, 283: 1–11

Flores R M (2013). Coal and Coalbed Gas. Amsterdam: Elsevier Inc

Gao F, Tang L, Zhou K, Zhang Y, Ke B (2018). Mechanism analysis of liquid carbon dioxide phase transition for fracturing rock masses. Energies, 11(11): 1–12

He B, Liu J, Zhao P, Wang J (2021). PFC^{2D}-based investigation on the mechanical behavior of anisotropic shale under brazilian splitting containing two parallel cracks. Front Earth Sci, 15(4): 803–816

Hodot B B (1966). Coal and Gas Outburst. Beijing: China Industry Press

Hu G, He W, Sun M (2018). Enhancing coal seam gas using liquid CO_2 phase-transition blasting with cross-measure borehole. J Nat Gas Sci Eng, 60: 164–173

Hu S B, Pang S G, Yan Z Y (2019). A new dynamic fracturing method: deflagration fracturing technology with carbon dioxide. Int J Fract, 220(1): 99–111

Jaimes M G, Castillo R D, Mendoza S A (2012). High energy gas fracturing: a technique of hydraulic prefracturing to reduce the pressure losses by friction in the near wellbore—a colombian field application. In: SPE Latin America and Caribbean Petroleum Engineering Conference. Mexico: Onepetro, 1–2

Karacan C Ö, Ruiz F A, Cotè M, Phipps S (2011). Coal mine methane: A review of capture and utilization practices with benefits to mining safety and to greenhouse gas reduction. Int J Coal Geol, 86(2-3): 121-156

Li J, Li B, Wang Z, Ren C, Yang K, Gao Z (2021). A permeability model for anisotropic coal masses under different stress conditions. J Petrol Sci Eng, 198: 1–10

Li Q Y, Liu X X, Wu Z Y, Xie X F (2018). Application of liquid CO_2 phase change rock breaking technology in metro foundation pit excavation. J Railw Sci Eng, 15(1): 164–169

Liao Z, Liu X, Song D, He X, Nie B, Yang T, Wang L (2021). Micro-structural damage to coal induced by liquid CO_2 phase change fracturing. Nat Resour Res, 30(2): 1613–1627

Liu J, Xie L, Elsworth D, Gan Q (2019). CO_2/CH_4 competitive adsorption in shale: implications for enhancement in gas production and reduction in carbon emissions. Environ Sci Technol, 53(15): 9328–9336

Liu J, Yao Y, Liu D, Elsworth D (2017). Experimental evaluation of CO_2 enhanced recovery of adsorbed-gas from shale. Int J Coal Geol, 179: 211–218

Liu Q, Cheng Y (2014). Measurement of pressure drop in drainage boreholes and its effects on the performance of coal seam gas extraction: a case study in the Jiulishan Mine with strong coal and gas outburst dangers. Nat Hazards, 71(3): 1475–1493

Liu Y, Li M, Yin G, Zhang D, Deng B (2018). Permeability evolution of anthracite coal considering true triaxial stress conditions and structural anisotropy. J Nat Gas Sci Eng, 52: 492–506

Lu J, Yin G Z, Zhang D M, Gao H, Li C, Li M (2020). True triaxial strength and failure characteristics of cubic coal and sandstone under different loading paths. Int J Rock Mech Min Sci, 135: 1–15

Lu T, Wang Z, Yang H, Yuan P, Han Y, Sun X (2015). Improvement of coal seam gas drainage by under-panel cross-strata stimulation using highly pressurized gas. Int J Rock Mech Min Sci, 77: 300–312

Lu Z, Jia Y, Zhou J, He P, Li M, Song Z, Cai X (2022). The permeability alternation of shale fractures due to Sc-CO_2 soaking: implications for Sc-CO_2 fracturing and deep CO_2 sequestration in shale reservoirs. Adv Mater Sci Eng, 2022: 1–12

Peng S, Zhou Y (2008). Discussion on models for gas leakage and diffusion. Gas & Heat, 28(11): 39-42 (in Chinese)

Qin C, Jiang Y, Zhou J, Song X, Liu Z, Li D, Zhou F, Xie Y, Xie C (2021). Effect of supercritical CO_2 extraction on CO_2/CH_4 competitive adsorption in Yanchang shale. Chem Eng J, 412: 1–16

Qin Y, Moore T A, Shen J, Yang Z, Shen Y, Wang G (2018). Resources and geology of coalbed methane in China: a review. Intern Geo Rev, 60(1): 1–36

Sampath K, Perera M, Elsworth D, Matthai S, Ranjith P G, Li D Y (2021). Discrete fracture matrix modelling of fully-coupled CO_2 flow – deformation processes in fractured coal. Intern J Rock Mechan Mining Sci, 138: 1–12

Vishal V, Ranjith P G, Singh T N (2015). An experimental investigation on behaviour of coal under fluid saturation, using acoustic emission. J Nat Gas Sci Eng, 22(1): 428–436

Wang D, Zeng F, Wei J, Zhang H, Yan W, Qiang W (2021). Quantitative analysis of fracture dynamic evolution in coal subjected to uniaxial and triaxial compression loads based on industrial CT and fractal theory. J Petrol Sci Eng, 196: 1–16

Wang H F, Cheng Y P, Wang L (2012). Regional gas drainage techniques in Chinese coal mines. Int J Min Sci Technol, 22(6): 873–878

Wang L, Liu S M, Cheng Y, Yin G, Zhang D, Guo P (2017). Reservoir reconstruction technologies for coalbed methane recovery in deep and multiple seams. Intern J Min Sci Techn, 27(2): 277–284

Woodward J L, Mudan K S (1991). Liquid and gas discharge rates through holes in process vessels. J Loss Prev Process Ind, 4(3): 161–165

Yan F, Xu J, Peng S, Zou Q, Zhou B, Long K, Zhao Z (2020). Breakdown process and fragmentation characteristics of anthracite

subjected to high-voltage electrical pulses treatment. Fuel, 275: 1–9

Yang W, Wang H, Zhuo Q, Lin B, Zhang J, Lu C, Lin M (2019). Mechanism of water inhibiting gas outburst and the field experiment of coal seam infusion promoted by blasting. Fuel, 251(4): 383–393

Yu Q X, Cheng Y (2012). Gas Control in Coal Mine. Xuzhou: China University of Mining & Technology Press

Zhang D, Bai X, Yin G, Li S, He Q (2018). Mechanism of breaking and fracture expansion of liquid CO_2 phase change jet fracturing in low-permeability coal seam. J China Coal Soc, 43(11): 3154–3168 (in Chinese)

Zhang X, Zhang D, Chin J L, Yin G Z, Feng D,Liyanapathirana D S (2017). Damage evolution and post-peak gas permeability of raw coal under loading and unloading conditions. Transport Porous Media, 117(3): 465–480

Zhao P, He B, Zhang B, Liu J (2022). Porosity of gas shale: Is the NMR-based measurement reliable. Petrol Sci, 19(2): 509–517

Zhao Y, Kang T, Hu Y (1995). Permeability classification of coal seams in China. Int J Rock Mech Min Sci Geomech Abstr, 32(4): 365–369

Zheng S, Wang H, Li B, Cheng Y, Zhang X, Wang Z, Geng S, Wang Z, Chen P, Lv P, Shi Z (2022). The effect of leakage characteristics of liquid CO_2 phase transition on fracturing coal seam: applications for enhancing coalbed methane recovery. Fuel, 308: 1–14

Zhou B, Xu J, Peng S, Yan F, Cheng L (2021). Effects of geo-stress on the dynamic response of multi-physical field parameters during coal and gas outbursts under true triaxial stress. Intern J Rock Mech Mining Sci, 142(4): 1–12

Zhou B, Xu J, Yan F, Peng S, Cheng L (2020a). Effects of gas pressure on dynamic response of two-phase flow for coal–gas outburst. Powder Techn, 377(1): 55–69

Zhou S, Jiang N, He X, Luo X (2020b). Rock breaking and dynamic response characteristics of carbon dioxide phase transition fracturing considering the gathering energy effect. Energies, 13(6): 1–16